Electronic bond structure of the H_2^+ ion in a strong magnetic field: A study of the parallel configuration

U. Kappes and P. Schmelcher*

Theoretische Chemie, Physikalisch-Chemisches Institut der Universität Heidelberg, Im Neuenheimer Feld 253, D-69120 Heidelberg, Germany

A large number of magnetically dressed states of the hydrogen molecular ion for parallel internuclear and magnetic field axes are investigated. The numerical calculations of the molecular states and potential-energy curves in the fixed-nuclei approximation are based on a recently established and optimized atomic orbital basis set. We study electronic states within the range $0 \leq |m| \leq 10$ of magnetic quantum numbers and for several field strengths. In particular, we also investigate many excited states within a subspace for fixed magnetic quantum number and parity. In order to understand the influence of the magnetic field on the chemical bond of excited molecular states, we perform a detailed comparison of the electronic probability distributions and potential-energy curves in the field-free space with those in the presence of a magnetic field. As a major result we observe the existence of two different classes of strongly bound, i.e., stable, magnetically dressed states whose corresponding counterparts in the field-free space exhibit purely repulsive potential-energy curves, i.e., are unstable. Corrections which are going beyond the fixed-nuclei approach, i.e., the coupling of the center of mass to the electronic motion, as well as the mass corrections are investigated in order to ensure the physical validity of our results.

PACS number(s): 31.10.+z, 32.60.+i

I. INTRODUCTION

During the past 20 years the influence of a strong magnetic field on the properties of molecular systems has been studied in a number of articles. Most of these investigations were on the hydrogen molecular ion [1–18] and only a few works of predominantly qualitative character dealt with few-electron molecules [19–24]. In addition a study of light diatomic molecules in the extreme high field regime, where the so-called adiabatic approximation is applicable, has been performed very recently [25].

A detailed understanding of the behavior of the H_2^+ ion in a strong magnetic field is of fundamental interest: It will give us a general idea of the effects of an external field on the chemical bond. As examples of such effects, which were already observed for the ground state of the H_2^+ ion, we mention the contraction of the bond length, the increase of the dissociation energies with increasing magnetic field strength, and the changes in the topology of the electronic potential-energy surfaces. In the case of a diatomic molecule in a strong magnetic field, and in particular for the H_2^+ ion, the electronic energies are two-dimensional surfaces: They depend on the internuclear distance R as well as the angle Θ between the internuclear and magnetic field axes. The major part of the existing literature on the H_2^+ ion in a magnetic field focused only on the lowest excited states for parallel internuclear and magnetic field axes: By different numerical approaches it was possible to investigate the lowest electronic states with orbital angular momentum projections

$m = 0, -1, \ldots, -5$ for different magnetic field strengths [14,16–18]. In the case where the internuclear axis is inclined with respect to the magnetic field direction by an arbitrary, nonzero angle Θ, our knowledge is restricted to the three lowest states with gerade and ungerade parity [9,12,15,16].

All the above-mentioned investigations on the H_2^+ ion in strong magnetic fields are based on special choices of variational electronic wave functions which take into account the symmetry lowering due to the presence of the external magnetic field. They are only applicable to the one-electron problem and in each case are restricted to a certain range of field strengths. The only basis set method was given in Ref. [16]. However, this method is also confined to the one-electron problem. In view of the lack of a general method for the calculation of molecular properties in strong magnetic fields, a basis set of atomic orbitals has been established in Ref. [26]. These atomic orbitals are well suited to describe electronic molecular wave functions and spectra for arbitrary magnetic field strengths and for an arbitrary orientation of the molecule with respect to the direction of the magnetic field. In order to apply this basis set in *ab initio* calculations of electronic molecular spectra and wave functions the variational parameters of the underlying atomic orbitals have to be optimized. This has been done recently for the case of the hydrogen atom [27]. In a first application of this optimized atomic orbital basis set the lowest electronic states of the H_2^+ ion with the magnetic quantum numbers $m = 0, -1, \ldots, -10$ were investigated for a fixed field strength of $B = 1.0$ a.u. The results of these calculations were very promising and, in particular, it was shown that the $1\eta_u (m = -5), \ldots 1\mu_g (m = -10)$ states become bound by the influence of the external magnetic field [28]. In the absence of a magnetic field the

---

*Present address: Physics Department, University of California, Santa Barbara, CA 93106-9530.

potential-energy curves of the corresponding counterparts of these electronic states exhibit a purely repulsive behavior and the electronic states in field-free space are therefore unstable with respect to dissociation, i.e., unbound.

The aim of the present article is to investigate a large number of magnetically dressed excited states of the H$_2^+$ ion for several magnetic field strengths. We hereby restrict our investigation to the case of parallel internuclear and magnetic field axes. The numerical calculations of the potential-energy curves are performed with the aid of the above-mentioned optimized atomic orbital basis set. We will study excited electronic states for a variety of different magnetic quantum numbers and field strengths and, in particular, also many excited states within a manifold of states of fixed magnetic quantum number. The latter class of excited magnetically dressed states of the H$_2^+$ ion has not been considered in the literature so far. One further major goal of the present paper is to contribute to the understanding of the formation of a chemical bond in the presence of a strong magnetic field.

Our investigation of the electronic structure of the H$_2^+$ ion is based on the fixed-nuclei approach. However, because of the finite mass of the nuclei, the full three-body problem of the charged H$_2^+$ system in an external magnetic field contains mass correction terms as well as an intrinsic coupling of the motion of the center of mass to the electronic motion. In order to ensure that our fixed-nuclei approach is valid for the magnetically dressed electronic states investigated, we will calculate the corresponding coupling terms and will estimate the order of magnitude of the mass correction terms.

The paper is organized as follows. In Sec. II we introduce and discuss the transformed full three-body Hamiltonian of the H$_2^+$ ion in a magnetic field. In Sec. III we briefly describe our method for the calculation of the molecular wave functions and electronic potential-energy surfaces. Since we investigate the influence of a strong magnetic field on the electronic structure of the H$_2^+$ ion we have to compare the magnetically dressed states with their corresponding counterparts in the absence of a magnetic field. Section IV, therefore, contains a discussion of the correlation of the electronic states of the H$_2^+$ ion in field-free space and their corresponding magnetically dressed counterparts. In Sec. V we present and analyze the results of our large scale computations on the H$_2^+$ ion in a strong magnetic field. We remark that atomic units will be used throughout the article.

II. THE HAMILTONIAN OF THE H$_2^+$ ION

The general problem we are concerned with is the motion of an electron and two protons under the influence of their mutual Coulomb interaction in the presence of an external homogeneous magnetic field. Due to the nonzero net charge of the H$_2^+$ system, the two components of the so-called pseudomomentum perpendicular to the magnetic field vector do not commute [29]. Therefore it is in principle not possible to perform a complete pseudoseparation of the center of mass motion, which means that the center of mass coordinates cannot be completely eliminated from the Hamiltonian. Nevertheless, it was shown in the literature [30–32] that the total Hamiltonian can be transformed to a particularly appealing form: the resulting Hamiltonian reflects the physically intuitive idea of the cyclotron motion of the center of mass which is perturbed by the coupling to the electronic degrees of freedom. For our case of the H$_2^+$ ion the above-mentioned nonrelativistic Hamiltonian takes on the following appearance:

$$H = H_{\text{c.m.}} + H_c + H_e + H_n + V(\mathbf{r}, \mathbf{R}) , \tag{1}$$

with

$$H_{\text{c.m.}} = \frac{1}{2M} \left[\mathbf{P}_{\text{c.m.}} - \frac{Q}{2} [\mathbf{B} \times \mathbf{R}_{\text{c.m.}}] \right]^2 , \tag{1a}$$

$$H_c = \frac{1}{M} \left[1 + \frac{1}{M} \right] \left[\mathbf{P}_{\text{c.m.}} - \frac{Q}{2} [\mathbf{B} \times \mathbf{R}_{\text{c.m.}}] \right] \cdot [\mathbf{B} \times \mathbf{r}] , \tag{1b}$$

$$H_e = \frac{1}{2} \left[\mathbf{p} + \frac{1}{2} [\mathbf{B} \times \mathbf{r}] + \frac{Q}{2} \frac{1}{M^2} [\mathbf{B} \times \mathbf{r}] \right]^2$$
$$+ \frac{1}{2M_0} \left[\mathbf{p} - \frac{1}{2} \left[1 + \frac{Q}{M} \frac{M + M_0}{M} \right] [\mathbf{B} \times \mathbf{r}] \right]^2 , \tag{1c}$$

$$H_n = \frac{2}{M_0} \left[\mathbf{P} - \frac{1}{4} [\mathbf{B} \times \mathbf{R}] \right]^2 , \tag{1d}$$

where M and M_0 denote the total mass of the ion and the total mass of nuclei, respectively. The vectors $\mathbf{R}_{\text{c.m.}}$, $\mathbf{P}_{\text{c.m.}}$ are the center of mass coordinate and its conjugated momentum, respectively. $\mathbf{r}$ and $\mathbf{R}$ are the relative coordinates of the electron and the distance vector of the nuclei, respectively, and $\mathbf{p}$, $\mathbf{P}$ are their corresponding conjugated momenta. As the origin of the internal coordinate system we have chosen the center of mass of nuclei. Q denotes the net charge of the ion, i.e., in our case of the H$_2^+$ ion $Q = 1$. For the vector potential we have adopted the symmetric gauge $\mathbf{A}(\mathbf{r}) = \frac{1}{2} [\mathbf{B} \times \mathbf{r}]$. $V(\mathbf{r}, \mathbf{R})$ contains all Coulomb interaction terms of the electron and the nuclei.

The Hamiltonian $H_{\text{c.m.}}$ in Eq. (1a) contains only the center of mass degrees of freedom and describes the collective motion of the ion by the approximation of a free pseudoparticle with the charge $Q = 1$ and mass M in a homogeneous magnetic field. The operator H_c couples the collective motion with the electronic degrees of freedom. It represents a motional Stark term with a rapidly changing electric field of intrinsic dynamical origin. This coupling term H_c can, in principal, mix up heavily the center of mass and electronic motion [31]. Therefore the center of mass motion of the molecular ion can deviate strongly from the zeroth-order Landau orbital motion given by $H_{\text{c.m.}}$. In particular, it is possible that the ion changes its state of collective and electronic motion via the coupling term H_c. Since an ion in a homogeneous magnetic field possesses a zero-point Landau energy the coupling term is an inherent property of the center of

mass motion of the ion in a magnetic field. This is in contrast to the case of a neutral molecule where the influence of the collective motion on the internal motion is given by a motional Stark effect with a constant electric field which vanishes in the special case of zero pseudomomentum [32–34]. We remark that the Hamiltonian H_c couples in the general case of a heteronuclear molecular ion the center of mass motion to all internal degrees of freedom, i.e., to the electronic as well as the nuclear degrees of freedom. Only for the special case of a homonuclear molecular ion, in particular the H_2^+ ion, do the coupling terms involve merely the electronic degrees of freedom [32].

The operator H_e in Eq. (1c) describes the motion of the single electron. Due to the finite nuclear mass this Hamiltonian contains a series of mass correction terms. They are proportional to powers of the mass ratio of the electron to nuclear mass. Finally, the Hamiltonian H_n represents the kinetic energy of the nuclear relative motion.

Since we want to study the electronic structure of the H_2^+ ion we have to separate the electronic and nuclear motion by an adiabatic approximation. The Born-Oppenheimer approximation in the presence of a magnetic field has, including all mass correction terms due to the finite mass of the nuclei, been investigated for neutral systems in detail in Refs. [32,35] and for molecular ions in Ref. [36]. For the present investigation we choose as a zeroth-order approach for the electronic Hamiltonian the fixed-nuclei Hamiltonian, i.e., we assume infinitely heavy nuclei. Theoretical considerations going beyond the fixed-nuclei approach, i.e., including mass correction terms or effects due to the Hamiltonian H_c, are given below. The justification of our assumption of infinitely heavy nuclei is given in Sec. V A 5 where we present the results of an explicit numerical evaluation of the corresponding correction terms for the electronic states and field strengths considered.

The fixed-nuclei electronic Hamiltonian (H_{fix}) we use in the present investigation can be obtained by locating the two protons at the fixed positions $\pm R/2$ on the z axis, which is taken to point along the direction of the magnetic field. For the explicit form as well as the symmetries of this well-known Hamiltonian we refer the reader to Refs. [27,28] and in particular to Ref. [40]. The eigenfunctions of the resulting electronic fixed-nuclei Schrödinger equation will be labeled $n\sigma$ (σ for $m=0$), $n\pi$ (π for $m=-1$), etc. The label n indicates the degree of excitation within the manifold of states of a given magnetic quantum number. An additional subscript g or u characterizes the parity of the orbitals.

The eigenvalues $\varepsilon(R)=\varepsilon^{nmP}(R)$ of the fixed-nuclei Hamiltonian H_{fix} do include the nucleus-nucleus Coulomb repulsion but not the threshold energy ε_{th} which is for an arbitrary negative magnetic quantum number m given by the lowest energy of a free electron in a magnetic field, i.e., $\varepsilon_{\text{th}}=B/2$. In order to shift the ionization threshold to zero energy we have to subtract the threshold energy ε_{th} from the eigenvalues $\varepsilon^{nmP}(R)$, i.e., we define $\varepsilon_T^{nmP}(R)=\varepsilon^{nmP}(R)-\varepsilon_{\text{th}}$.

In the remaining part of this section we give some theoretical considerations going beyond the fixed-nuclei approach. The results will be the basis for our later justification (see Sec. V A 5) and improvement of the approximation of infinitely heavy nuclei. Let us first investigate the importance of the coupling term H_c between the collective motion of the ion and the electronic degrees of freedom. To this end we expand the total wave function in a series of products of Landau orbitals, which are eigenfunctions of the Hamiltonian $H_{\text{c.m.}}$, and the electronic wave functions, which are eigenfunctions of H_e. The corresponding total electronic Hamiltonian which takes into account the collective and electronic motion is the sum of the operators $H_{\text{c.m.}}$, H_c, and H_e. The off-diagonal matrix elements of the resulting Hamiltonian matrix take on the following structure:

$$\frac{1}{M}\left[1+\frac{1}{M}\right]\left\langle\Phi_{N\mu}^L\left|\mathbf{P}_{\text{c.m.}}-\frac{Q}{2}[\mathbf{B}\times\mathbf{R}_{\text{c.m.}}]\right|\Phi_{N'\mu'}^L\right\rangle\cdot\left\langle\Psi^{nmP}\left|[\mathbf{B}\times\mathbf{r}]\right|\Psi^{n'm'P'}\right\rangle, \tag{2}$$

where $(N\mu)$ and $(N'\mu')$ denote the quantum numbers of the Landau orbitals and (nmP), $(n'm'P')$ are the quantum numbers of the electronic magnetically dressed states. These matrix elements couple different states consisting of a product of certain Landau orbitals of the center of mass motion and electronic eigenstates to H_e. It has been shown in the literature [31] that the matrix elements (2) can be reduced to a product of dipole matrix elements between different Landau orbitals and dipole matrix elements between different electronic eigenstates. For the estimations of the importance of the coupling term H_c we focus on a coupled two-state problem. The quantity κ, which is the relevant measure for the strength of the coupling, is the square of the ratio of the absolute value of the coupling matrix elements and the energy gap between the considered states (this can be seen by second-order perturbation theory):

$$\kappa=4\left[\frac{1}{M}\left[1+\frac{1}{M}\right]\right]^2\frac{\left|\left\langle\Phi_{N\mu}^L\left|\mathbf{P}_{\text{c.m.}}-\frac{Q}{2}[\mathbf{B}\times\mathbf{R}_{\text{c.m.}}]\right|\Phi_{N'\mu'}^L\right\rangle\cdot\left\langle\Psi^{nmP}\left|[\mathbf{B}\times\mathbf{r}]\right|\Psi^{n'm'P'}\right\rangle\right|^2}{[E_{N\mu}+\varepsilon_T^{nmP}(R)-E_{N'\mu'}-\varepsilon_T^{n'm'P'}(R)]^2}, \tag{3}$$

where $E_{N\mu}$ and $E_{N'\mu'}$ are the energies of the Landau states $\Phi_{N\mu}^L$ and $\Phi_{N'\mu'}^L$, respectively. If κ is much smaller than unity the coupling between different states of the collective and electronic motion is negligible and no relevant mixing occurs. In Sec. V A 5 we will present numerically calculated values of κ for low-lying Landau orbitals and our investigated magnetically dressed states of the H_2^+ ion.

Finally we briefly comment on the mass correction terms of the electronic Hamiltonian H_e. To the lowest order of the electron to the nuclear mass ratio $(1/M)$ the mass corrections of H_e can be included in the fixed-nuclei Hamiltonian by simply replacing the mass of the electron by the reduced masses μ and μ', i.e., the electronic Hamiltonian of the H_2^+ ion including first-order mass correction terms reads as follows:

$$H_e' = \frac{1}{2\mu}\mathbf{p}^2 + \frac{1}{2\mu'}BL_z + \frac{1}{8\mu}B^2(x^2+y^2) + V(\mathbf{r},\mathbf{R}) , \qquad (4)$$

where $\mu = M_0/(M_0+1)$ and $\mu' = M_0/(M_0-1)$.

Let us now proceed to solve the fixed-nuclei electronic Schrödinger equation. For that purpose we have to build up the electronic magnetically dressed molecular wave functions from the optimized atomic orbitals, thereby respecting the symmetries in the presence of the external magnetic field. In Sec. III we describe the construction of the molecular orbitals as well as the ab initio method for the calculation of the potential-energy surfaces of the H_2^+ ion.

III. NUMERICAL METHOD
FOR THE CALCULATION OF THE ELECTRONIC
FIXED-NUCLEI SPECTRUM OF THE H_2^+ ION

The basis set of atomic orbitals which are a key ingredient for our numerical calculation of the spectrum and wave functions of the hydrogen molecular ion were established in Ref. [26]. For a detailed description of these atomic orbital basis functions as well as the optimization procedure of the nonlinear variational parameters of these orbitals we refer the reader to Ref. [27]. The final form of our atomic orbitals takes on the following appearance:

$$\phi_n(\mathbf{r},\underline{\alpha},\mathbf{R}_{1/2}) = x^{n_x}y^{n_y}(z \mp R/2)^{n_z}$$
$$\times \exp\{-\alpha(x^2+y^2)-\beta(z \mp R/2)^2\} , $$
$$(5)$$

where α, β represent the optimized variational parameters and $\mathbf{R}_1 = -\mathbf{R}_2 = \mathbf{R}/2$ with $\mathbf{R} = R(0,0,1)^T$.

In order to solve the electronic fixed-nuclei Schrödinger equation $H_{fix}\Psi^{mP} = \varepsilon^{mP}\Psi^{mP}$ we expand the electronic wave function Ψ^{mP} in terms of nonorthogonal molecular orbitals.

$$\Psi^{mP} = \sum_i c_i \Phi_i^{mP} . \qquad (6)$$

The molecular orbitals Φ_i^{mP} are built up by the corresponding optimized atomic orbitals (5). They reflect the symmetries of the underlying system, i.e., they are eigenfunctions of the parity operator P and the z component of

the angular momentum operator L_z. The method of construction of the molecular eigenfunctions Φ_i^{mP} to the parity as well as angular momentum operator by using the linear combination of atomic orbitals (LCAO) method is briefly described in the Appendix.

The resulting generalized eigenvalue problem reads as follows:

$$(\underline{H}_{fix} - \varepsilon \underline{S})\mathbf{c} = 0 , \qquad (7)$$

where the Hamiltonian matrix $\underline{H}_{fix}$ is real and symmetric and the overlap matrix $\underline{S}$ is real, symmetric, and positive definite. The vector $\mathbf{c}$ comprises the expansion coefficients c_i. The matrix elements $(\underline{H}_{fix})_{ij}$ and $(\underline{S})_{ij}$ are linear combinations of matrix elements with respect to the optimized atomic orbitals. The latter matrix elements have been calculated in Ref. [26]. Closed form analytical expression could be obtained for all matrix elements except the electron-nucleus attraction integrals. These three center integrals could be reduced to a smooth one-dimensional integration which was computed numerically by using a Tschebyscheff-polynomial quadrature. For the numerical solution of the eigenvalue problem (7) we used standard methods.

IV. CORRELATION OF THE FIELD-FREE
AND MAGNETICALLY DRESSED STATES

In order to analyze the influence of the external magnetic field on the molecular electronic states of the H_2^+ ion we have to compare the potential-energy curves of the considered states in a magnetic field with their corresponding counterparts in the absence of the field. We thereby have to ensure that the magnetically dressed molecular states can be related to the corresponding field-free states in a unique way. For parallel internuclear and magnetic field axes, which is the case we exclusively consider in the present paper, the lowest state of a given manifold m^P can be associated with the likewise lowest state with the same magnetic quantum number m and parity P in the field-free case [27,28]. For example, the magnetically dressed states of the H_2^+ ion $1\sigma_g, 1\pi_u, 1\delta_g, \ldots$ evolve from the $1s\sigma_g, 2p\pi_u, 3d\delta_g, \ldots$ field-free states in a definite way. For excited states of a given subspace m^P such a one-to-one correlation between the magnetically dressed molecular states and the states in the field-free case does not exist. The reason for this fact is the breakdown of the noncrossing rule for the case of the H_2^+ ion in the absence of a magnetic field [37,38]: Since there exists in addition to the spatial symmetries also a phase-space symmetry for the H_2^+ ion in the field-free space, crossings of potential-energy curves with the same spatial symmetries are allowed. If we switch on a magnetic field the phase-space symmetry is destroyed and the noncrossing rule holds. As a consequence we are, in general, not able to relate an excited magnetically dressed molecular state of a given subspace m^P to only one molecular state in the field-free case. However, for the manifolds m^P considered in the present paper, the potential-energy curves of the first two excited states of each manifold exhibit in the absence of a magnetic field only one crossing. They cross each other for small values

of the internuclear distance, i.e., in the strongly repulsive regions which correspond to nuclear configurations close to the united atom limit. Apart from this crossing the first two excited states of each manifold m^P are energetically well separated. This energetic separation is maintained if we switch on a magnetic field. It is therefore reasonable to compare the properties of the first two excited states of the H^{2+} ion in the field-free case in each subspace m^P with those of the first and second magnetically dressed states of the H_2^+ ion with the same magnetic quantum number m and parity P. For example, the molecular states $3d\sigma_g$ and $2s\sigma_g$ in the absence of a magnetic field correspond to the magnetically dressed states $2\sigma_g$ and $3\sigma_g$, respectively. For higher excited states the large number of crossings, in particular also close to the equilibrium internuclear distances, does not allow for an identification of the individual states as a function of the field strength.

V. RESULTS AND DISCUSSION

In the following we present and discuss the results of our extensive numerical calculations which have been obtained by using the above-described *ab initio* method. First of all we will investigate different electronic states of the H_2^+ ion in a strong magnetic field with the same

magnetic quantum number but with increasing degree of excitation. We will study the potential-energy curves of the magnetically dressed states and, if possible, compare them to their corresponding counterparts in the absence of a magnetic field. In Figs. 1(a)–1(c) the potential-energy curves of the four lowest so-called "bonding" as well as "antibonding" states of the H_2^+ ion in a magnetic field of the strength 1.0 are shown for the manifolds with the magnetic quantum numbers $m = 0, -1, -2$, respectively. Since the two lowest states of the manifold $m = 0$, i.e., the $1\sigma_{g/u}$ states, are energetically well separated from all other states in the subspace $m = 0$, they have been omitted in Fig. 1(a).

A. The magnetically dressed bonding states

Let us first consider the properties of the bonding states, i.e., of the $2\sigma_g, 3\sigma_g, \ldots, 1\pi_u, 2\pi_u, \ldots, 1\delta_g, 2\delta_g, \ldots$, states. Analogous to the ground state $1\sigma_g$ of the H_2^+ ion, all potential-energy curves of these electronic states exhibit an attractive behavior with a well-pronounced potential well. The depths of these potential wells, i.e., the dissociation energies of the considered states, are roughly of the order of magnitude of 10^{-2}. As examples we mention the $2\sigma_g, 3\sigma_g, 4\sigma_g$ states of the man-
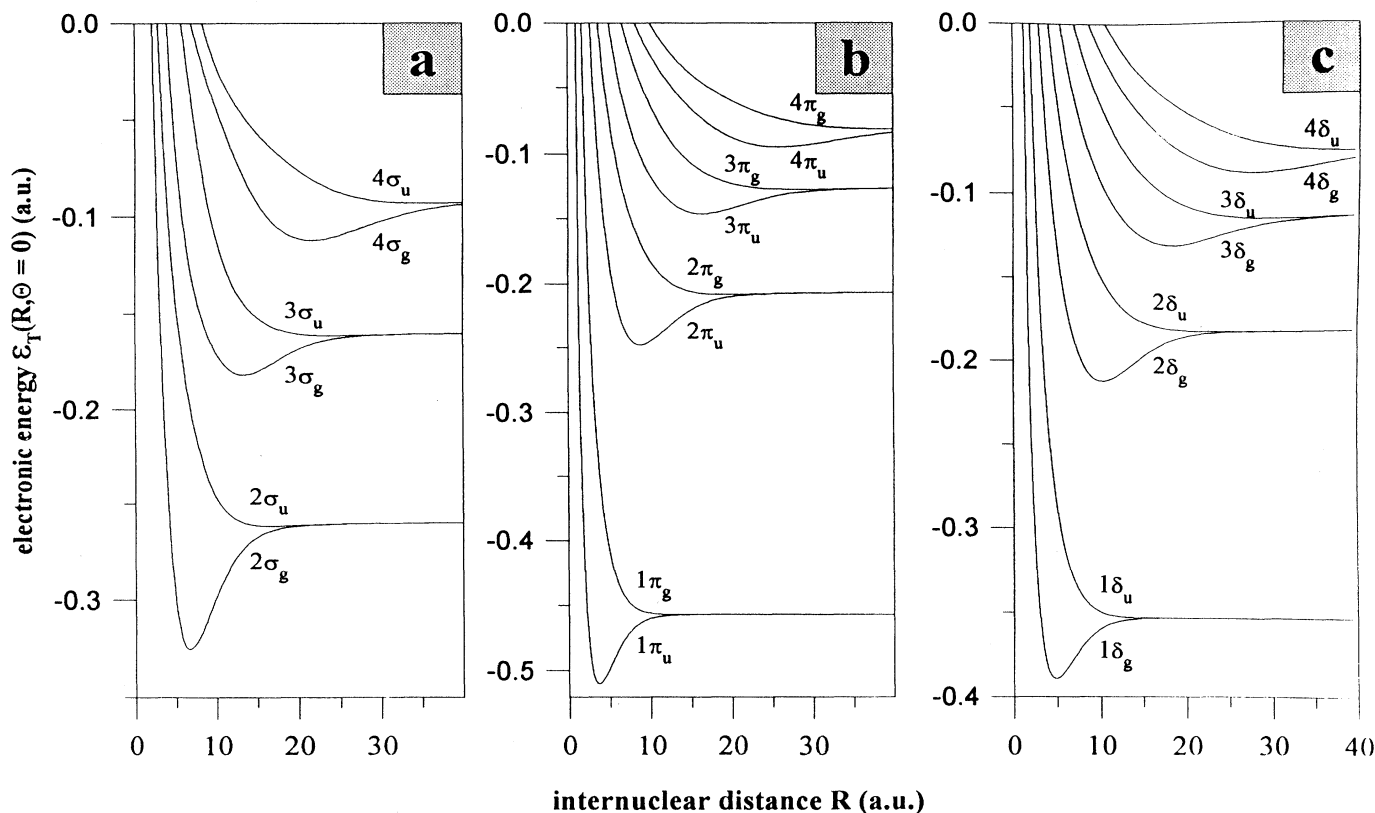
FIG. 1. Total electronic energies (including the nuclear repulsion energy) of excited "bonding" and "antibonding" states of the H_2^+ ion in a strong magnetic field $B = 1.0$ illustrated as functions of the internuclear distance R. (a) The electronic potential curves of the first six excited states of the σ manifold $(m = 0)$, (b) and (c) show the eight lowest states of the $\pi(m = -1)$ and $\delta(m = -2)$ manifold, respectively.

ifold $m=0$ whose dissociation energies are 6.552×10^{-2}, 2.209×10^{-2}, and 2.203×10^{-2}, respectively. For a given magnetic quantum number m the width of the potential well increases with increasing degree of excitation of the electronic state considered. In addition a strong increase of the equilibrium distances of the magnetically dressed states of a given manifold m with increasing excitation can be observed. Let us again consider as an example the

σ_g subspace. For the lowest state $1\sigma_g$ of this manifold (which is the global ground state of the H_2^+ ion) we find an equilibrium distance of 1.76. For the excited states $2\sigma_g, 3\sigma_g$, and $4\sigma_g$ the equilibrium distances are 6.64, 13.37, and 21.56, respectively. A complete list of the equilibrium distances as well as the dissociation energies of the above-mentioned states of the H_2^+ ion in a magnetic field of $B=1.0$ is given in Table I(b).

TABLE I. The equilibrium internuclear distances R_{eq}, the electronic energy at the equilibrium distance $\varepsilon_T(R_{eq})$, and the dissociation energies ε_D of the bonding $\sigma, \pi, \ldots, \gamma$ states $(m=0, \ldots, -4)$ of the hydrogen molecular ion (a) in the absence of a magnetic field and (b) in the presence of a magnetic field with $B=1.0$. In the field-free case the potential-energy curves of the corresponding states exhibit small humps. The values of these local energy maxima ε_{max} are also given.

(a)

State	R_{eq}	$\varepsilon_T(R_{eq})$	ε_{max}	ε_D
$1s\sigma_g$	2.03	-5.9876×10^{-1}		1.012×10^{-1}
$3d\sigma_g$	8.80	-1.7468×10^{-1}		4.978×10^{-2}
$2s\sigma_g$			purely repulsive	
$5g\sigma_g$	23.90	-7.8129×10^{-2}		2.258×10^{-2}
$2p\pi_u$	8.00	-1.3424×10^{-1}	-1.2469×10^{-1}	9.550×10^{-3}
$4f\pi_u$	19.00	-7.1128×10^{-2}		1.558×10^{-2}
$3p\pi_u$			purely repulsive	
$6h\pi_u$	39.00	-4.1558×10^{-2}		1.031×10^{-2}
$3d\delta_g$	18.00	-5.6877×10^{-2}	-5.6262×10^{-2}	1.614×10^{-3}
$5g\delta_g$	32.00	-3.7844×10^{-2}		6.593×10^{-3}
$4d\delta_g$			purely repulsive	
$7i\delta_g$	58.00	-2.5517×10^{-2}		5.517×10^{-3}
$4f\phi_u$	33.00	-3.1191×10^{-2}	-3.0913×10^{-2}	2.783×10^{-4}
$6h\phi_u$	49.00	-2.3219×10^{-2}		3.219×10^{-3}
$5g\gamma_g$	53.00	-1.9656×10^{-2}	-1.9633×10^{-2}	2.278×10^{-5}
$7i\gamma_g$	68.00	-1.5576×10^{-2}		1.687×10^{-3}

(b)

State	R_{eq}	$\varepsilon_T(R_{eq})$	ε_D
$1\sigma_g$	1.76	-9.7321×10^{-1}	1.437×10^{-1}
$2\sigma_g$	6.64	-3.2536×10^{-1}	6.552×10^{-2}
$3\sigma_g$	13.37	-1.8232×10^{-1}	2.209×10^{-2}
$4\sigma_g$	21.56	-1.1221×10^{-1}	2.203×10^{-2}
$1\pi_u$	3.68	-5.1007×10^{-1}	5.354×10^{-2}
$2\pi_u$	8.82	-2.4795×10^{-1}	4.139×10^{-2}
$3\pi_u$	16.38	-1.4621×10^{-1}	2.075×10^{-2}
$4\pi_u$	25.85	-9.4781×10^{-2}	1.545×10^{-2}
$1\delta_g$	4.87	-3.8944×10^{-1}	3.641×10^{-2}
$2\delta_g$	10.29	-2.1272×10^{-1}	3.276×10^{-2}
$3\delta_g$	18.31	-1.3027×10^{-1}	1.873×10^{-2}
$4\delta_g$	28.39	-8.6559×10^{-2}	1.330×10^{-2}
$1\phi_u$	5.79	-3.2847×10^{-1}	2.851×10^{-2}
$2\phi_u$	11.45	-1.9095×10^{-1}	2.796×10^{-2}
$1\gamma_g$	6.55	-2.8995×10^{-1}	2.377×10^{-2}
$2\gamma_g$	12.43	-1.7559×10^{-1}	2.476×10^{-2}

1. The potential-energy curves
of the manifolds $|m| \leq 2$

In order to analyze the influence of the external magnetic field on the potential-energy curves of the H_2^+ ion we representatively compare the three lowest so-called "bonding" states of the subspace $m = 0$ in the absence of a magnetic field with those in the presence of a magnetic field with $B = 1.0$.

Let us first consider the potential-energy curves of the σ_g states in the absence of a magnetic field. The energy curves of the lowest states with the magnetic quantum numbers $|m| \leq 4$ are well known since the early investigations of Bates and co-workers [39]. However, for a consistent comparison of the corresponding states with their counterparts in the presence of a magnetic field, we have recalculated the wave functions and spectra in field-free space with our optimized atomic orbital basis set. The data on the H_2^+ ion in field-free space given in the present paper are therefore results of our own basis set calculations. The eigenenergies obtained show an overall accuracy of about 0.1% compared to the corresponding very accurate values of Bates and co-workers [39]. The ground state $1s\sigma_g$ and the first excited state $3d\sigma_g$ exhibit well-pronounced potential wells located around 2.03 and 8.80, respectively. The corresponding dissociation energies are 1.012×10^{-1} and 4.978×10^{-2}, respectively. In contrast to the first excited state the second excited state

$2s\sigma_g$ exhibits a purely repulsive behavior [a complete list of equilibrium distances and dissociation energies for the electronic states in field-free space for all subspaces m^P considered in the present paper is given in Table I(a)]. The absence of an attractive part in the potential-energy curve of the $2s\sigma_g$ state simply means that it is unstable with respect to the dissociation $H_2^+ \rightarrow H + p$.

In the case of the presence of a magnetic field of $B = 1.0$ the corresponding potential-energy curves of the $1\sigma_g$, $2\sigma_g$, and $3\sigma_g$ states exhibit, as we mentioned above, well-pronounced potential wells. For the first two states $1\sigma_g$ and $2\sigma_g$ we obtain compared to the field-free quantities a decrease of the bond lengths of about 13.3% and 24.5% and an increase of the dissociation energies of approximately 42% and 31.6%, respectively. The $3\sigma_g$ state, whose counterpart $2s\sigma_g$ in the field-free case exhibits a purely repulsive energy curve, shows now, in the presence of a magnetic field, an attractive potential-energy curve. In order to understand these drastic changes of the potential-energy curves let us consider the electronic probability density distributions of the lowest three states of the σ_g manifold in the absence and presence of a magnetic field.

2. Electronic probability density distributions

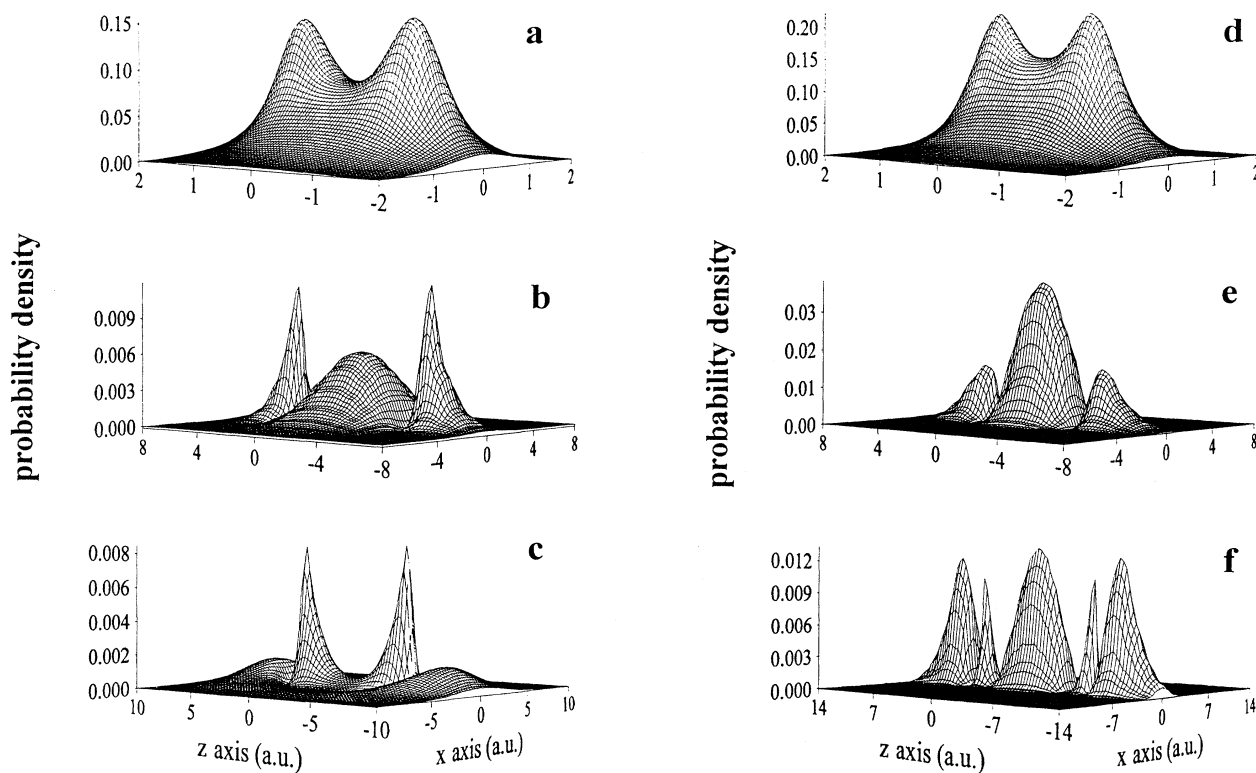In Fig. 2 the electronic probability density distributions of the lowest three σ_g states in the field-free case

FIG. 2. The electronic probability density distributions of the three lowest "bonding" states of the σ_g manifold ($m = 0$) of the H_2^+ ion in the absence of a magnetic field are shown in (a)–(c). (d)–(f) show the corresponding states in the presence of a magnetic field. The electronic density distributions of the "field-free states" $1s\sigma_g$ (a) and $3d\sigma_g$ (b) and of the magnetically dressed states $1\sigma_g$ (d), $2\sigma_g$ (e), and $3\sigma_g$ (f) are plotted for the corresponding equilibrium distances. The density of the "field-free state" $2s\sigma_g$ (c), which exhibits a purely repulsive potential-energy curve, is shown for an internuclear distance 8.80.

[Figs. 2(a)–2(c)] are opposed to their corresponding counterparts in the presence of a magnetic field $B = 1.0$ [Figs. 2(d)–2(f)]. All density distributions $n(x,z) = |\Psi(x,z)|^2$ of Fig. 2 are plotted in the x-z plane. Let us first discuss the probability distribution of the well-known $1s\sigma_g$ state which is illustrated in Fig. 2(a) for the equilibrium distance of 2.03. The distribution exhibits two maxima which are located at the positions of the nuclei. Their absolute values are approximately 0.16. Between the two maxima the density decreases, i.e., the density distribution exhibits a saddle point with an absolute value of roughly 0.085 at the position $x = z = 0$. This relatively large probability of finding the electron between both nuclei leads to a screening of the nuclear charges by the electronic cloud and to the existence of a well-pronounced potential well in the potential-energy curve of the $1s\sigma_g$ state. If we switch on a magnetic field of $B = 1.0$ the density distribution of the $1\sigma_g$ state [see Fig. 2(d)], which is the magnetically dressed counterpart of the $1s\sigma_g$ state, shows an enhancement of the absolute values of the maxima (0.21), which are still located at the positions of the nuclei, and an increase of the density between both nuclei. The value at the saddle point is now about 0.16. The overall increase of the density distribution close to and in particular between both nuclei in the presence of a magnetic field leads to a more complete screening of the nuclear charges and in particular to a lowering of the potential energy. As a consequence the depth of the potential well in the corresponding potential-energy curve increases.

Next let us consider the density distribution for the $3d\sigma_g$ state ($B = 0$) and its counterpart the $2\sigma_g$ state for $B = 1.0$. The density distribution of the $3d\sigma_g$ state in field-free space is illustrated in Fig. 2(b) for the equilibrium distance of 8.80. The probability distribution exhibits three maxima along the internuclear line which are separated by nodes. The outer maxima ($n_{ext} \approx 9 \times 10^{-3}$) are peaked at the positions of the individual nuclei. The density around the inner maximum, which is located at the origin of the x-z plane, is more widely distributed and the inner maximum value itself is only about half of the absolute values of the outer maxima. The existence of a local maximum for the density between both nuclei leads to the existence of a potential well in the energy curve of the $3d\sigma_g$ state. In Fig. 2(e) the density distribution of the corresponding magnetically dressed state $2\sigma_g$ is presented for $B = 1.0$ and the corresponding equilibrium distance of 6.64. The values of the outer maxima, which are still located at the position of the nuclei, are now a little larger ($n_{ext} \approx 0.015$) but they no longer represent the global maxima of the density distribution. Instead we observe a strong increase of the density between the nuclei and the global maximum of the density ($n_{in} \approx 0.036$) is located at the origin. In addition the density distribution of the $2\sigma_g$ state for $B = 1.0$ [see Fig. 2(e)] is much more strongly localized in the vicinity of the internuclear axis than the density of the $3d\sigma_g$ state in field-free space [see Fig. 2(b)], i.e., the magnetic field also causes a contraction of the electronic cloud perpendicular to the internuclear axis.

The strong increase of the density distribution between

the nuclei for the $2\sigma_g$ state compared to the $3d\sigma_g$ state in the field-free space leads, however, only to a moderate increase of the corresponding dissociation energies of about 31.6%. The decrease of the bond length is of the same order of magnitude (24.5%). This picture changes if we consider the first excited states of the subspaces with nonvanishing magnetic quantum numbers ($|m| \geq 1$). In the latter case we obtain much more drastic relative changes of the dissociation energies as well as bond lengths if we pass from the field-free situation to the case of the presence of a magnetic field (see Tables I(a) and I(b) for a comparison of the corresponding data). The relative changes are bigger the larger the absolute value of the magnetic quantum number $|m|$ is. This fact is not very surprising since the binding energy of the underlying system decreases with increasing degree of excitation and the increasing magnetic interaction energies, therefore, dominate more and more. With the exception of a node line along the z axis which has its origin in the polynomial part $(x \pm iy)^{|m|}$ of the electronic wave function [see Eq. (A7)], the density distributions of the first excited states of the manifolds $\pi_u, \delta_g, \phi_u, \gamma_g, \ldots$ take on an appearance similar to the above-discussed distributions of the $3d\sigma_g$ and $2\sigma_g$ states. This statement holds for the case of the absence as well as presence of the magnetic field.

Let us finally consider how the probability density distribution of the second excited state of the σ_s manifold in the field-free case changes if we switch on a magnetic field $B = 1.0$. In Fig. 2(c) the probability distribution of the $2s\sigma_g$ state is illustrated for an internuclear distance of 8.80. We observe two sharp peaks, which are located at the positions of the nuclei and represent the global maxima ($n_{in} \approx 6.8 \times 10^{-3}$). In addition, the density distribution shows two further outer maxima which are separated by nodes from the global maxima. The density distribution around these outer maxima ($n_{ext} \approx 1.2 \times 10^{-3}$) is rather broad compared to the peaks at the positions of the nuclei. Similar to the $1s\sigma_g$ state, the probability distribution of the $2s\sigma_g$ state exhibits between the nuclei a saddle point ($n_{sad} \approx 4 \times 10^{-4}$). However, the relative difference between the values of the global maxima and the value at the saddle point is very large. This strong decrease of the density distribution between the two nuclei is the reason for the purely repulsive potential-energy curve of the $2s\sigma_g$ state, i.e., the very low probability of finding the electron between both nuclei does not allow for the formation of a chemical bond. In the presence of a magnetic field of $B = 1.0$ the density distribution of the corresponding $3\sigma_g$ state, given in Fig. 2(f) for the equilibrium distance of 13.37, takes on a very different appearance. The existence of an additional maximum located between both nuclei is most remarkable. Remember, in the field-free case [see Fig. 2(c)] we observe in this area a low-lying saddle point. This newly formed maximum, which is located at the origin, is also the global maximum of the density distribution. The peaks of the density distribution in the absence of a magnetic field, which were located at the positions of the nuclei, are still present and the two outer maxima, which were smooth and widely distributed in the field-free case, are now much more pronounced and peaked. In addition we observe a strong lo-

calization of the density distribution in the plane perpendicular to the magnetic field. The enhanced density between both nuclei leads to the existence of an attractive part in the potential-energy curve of the $3\sigma_g$ state. This behavior is, within our investigation of the electronic structure of the H_2^+ ion, generic for all second excited states with different magnetic quantum numbers m, whose field-free counterparts are the so-called "bonding" states. This means that not only the $2s\sigma_g$ state but also the $3p\pi_u$ and $4d\delta_g$ electronic states in the field-free space exhibit purely repulsive potential-energy curves [see Table I(a)] whereas their corresponding counterparts in the presence of a magnetic field of $B=1.0$, i.e., the $3\sigma_g, 3\pi_u, 3\delta_g$ states, show an attractive behavior of the potential-energy curves [see Table I(b)], i.e., a well-pronounced potential well. In particular the changes in the electronic probability density distribution due to the presence of a magnetic field are, with the exception of the occurrence of a node line along the magnetic field axis, for the $3\pi_u, 3\delta_g$ states similar to that observed for the $3\sigma_g$ state.

3. The ground states of the manifolds $4 \le |m| < 10$

After having studied the influence of the magnetic field on the properties of the so-called "bonding" excited states in the manifolds $\sigma_g, \pi_u, \delta_g$ we will in the following investigate the changes in the properties of the lowest states with increasing magnetic quantum number in the absence and presence of a magnetic field. According to our above discussion, the density distribution of the ground state of the H_2^+ ion exhibits in the absence of a magnetic field a saddle point between both nuclei [see Fig. 2(a)]. The density distributions of all other lowest states of the manifolds m^P possess, due to the polynomial structure $(x \pm iy)^{|m|}$ of the orbitals [see Eq. (A7)], a node line along the z axis. The following features are common to all ground states of the manifolds $\sigma_g, \pi_u, \delta_g, \phi_u, \gamma_g, \cdots$ in field-free space: The maxima of the electronic probability density occur roughly for values of the z coordinate which correspond to the positions of the nuclei whereas their distance from the z axis increases with increasing absolute value of the magnetic quantum number. Between the two maxima we observe a saddle point at $z=0$. However, with increasing magnetic quantum number the electronic probability density becomes more and more widely distributed. In particular, the values of the probability density close to the internuclear axis between the two nuclei become very small. Since the distribution of the probability density close to the internuclear axis between the nuclei is an indication of whether a potential well may exist for a certain state or not, it could be expected that the potential-energy curves of the lowest states with the quantum numbers m^P in field-free space exhibit, from a certain magnetic quantum number $|m|$ on, a purely repulsive behavior. And indeed, *only the electronic potential-energy curves of the above-mentioned states with magnetic quantum numbers $|m| \le 4$ are attractive,* i.e., possess a potential well while the potential-energy curves of the ground states with magnetic quantum numbers $|m| \ge 5$ exhibit purely repulsive behavior,

i.e., they are unstable with respect to the dissociation $H_2^+ \to H + p$ [28].

In the following we will investigate how the shapes of the potential-energy curves of these so-called "bonding" states change if we switch on a homogeneous magnetic field. For that purpose we consider the ground states $1\gamma_g, 1\eta_u, 1\iota_g, 1\varphi_u, 1\kappa_g, 1\lambda_u, 1\mu_g$ with the magnetic quantum numbers $4 \le |m| \le 10$. For a field strength of 0.01 we obtain for all of the above-mentioned states shallow wells in their potential-energy curves. With increasing magnetic field strength the potential wells become more and more pronounced and the corresponding equilibrium distances decrease rapidly. For a strong magnetic field with a field strength of $B=1.0$ we obtain for all states considered dissociation energies of the order of magnitude of 10^{-2} a.u. and equilibrium distances ranging from 6.55 for the $1\gamma_g$ state ($|m|=4$) to 9.80 for the $1\mu_g$ state ($|m|=10$) (a complete list of equilibrium distances as well as dissociation energies for the states with the magnetic quantum numbers $4 \le |m| \le 10$ is given for the field strengths 0.01, 0.1, and 1.0 in Table II).

In order to understand the drastic changes of the shape of the potential-energy curves of the considered so-called "bonding" ground states from the field-free case to the case of the presence of a magnetic field we representatively consider the electronic probability density distribution of the η_u state ($|m|=5$) in both cases. In Figs. 3(a) and 3(b) the density distribution of the $6h\eta_u$ state in the absence of a magnetic field and of the $1\eta_u$ state in the presence of a magnetic field with $B=1.0$ are illustrated, respectively. The probability density of the $6h\eta_u$ state in Fig. 3(a) is presented for an internuclear distance of 80.0. The maxima ($n_{\max} \approx 3 \times 10^{-6}$) of the density distribution occur for values of the z coordinate which correspond to the positions of the nuclei and are located roughly 30 a.u. away from the z axis. The saddle point of the density ($n_{\text{sad}} \approx 7 \times 10^{-7}$) occurs at $z=0$ and has a distance of roughly 40.0 a.u. from the internuclear axis. The purely repulsive behavior of the electronic potential curve for the $6h\eta_u$ state in the field-free case has, as we mentioned above, its origin in the low and widely distributed probability density. In the presence of a magnetic field the structure of the probability distribution of the $1\eta_u$ state, illustrated in Fig. 3(b) for the equilibrium distance 7.22, is completely different from that of the $6h\eta_u$ state in field-free space. The maxima of the density occur close to the internuclear axis at approximately $x=\pm3$ and at $z=0$. In the region defined by $-1.0 \le z \le 1.0$ and $x=\pm3$ the density shows, starting from its maximal value at $z=0$, only a very minor decrease. Apart from the decrease of the overall size of the molecule we also observe that the density is very much peaked in the direction of the x axis, which corresponds to the direction perpendicular to the magnetic field. The enhanced probability of finding the electron in the region close to the internuclear axis for z values between both nuclei leads, compared to the field-free situation, to a more complete screening of the nuclear charges and allows consequently for the formation of the observed well-pronounced potential well.

The above-discussed influence of a strong magnetic

field on the ground state of the η_u manifold is representative for all magnetically dressed ground states considered in the present paper (see Table II), i.e., the changes of the properties of the potential-energy curves as well as the changes of the corresponding probability density distributions of the ground states of the $\gamma_g, \ldots, \mu_g$ manifolds from field-free space to the presence of a magnetic field are analogous to those of the above-described η_u ground-state.

4. Existence of vibrational levels

So far we have investigated the properties of a large number of the so-called "bonding" adiabatic electronic states of the H_2^+ ion in the presence of a strong magnetic field. We, thereby, have shown that the adiabatic potential-energy curves of all magnetically dressed "bonding" states considered exhibit well-pronounced potential wells for a field strength of $B = 1.0$, in particular also those whose corresponding counterparts exhibit in field-free space a purely repulsive behavior. However, the existence of a potential well in the adiabatic potential-energy curves is a necessary but not sufficient condition for the formation of a stable molecular bond. In order to find out whether a certain magnetically dressed "bonding" state of the H_2^+ ion is stable with

respect to dissociation $H_2^+ \rightarrow H + p$, we have to ensure the existence of vibrational states in the corresponding potential wells. To this end we approximate the potential wells by a harmonic potential and estimate the ground-state energy of the nuclear motion in this harmonic potential well under the influence of the external magnetic field. In a rough approximation an upper limit of the vibrational ground-state energy is then given by the sum of the ground-state energy in the harmonic potential and the corresponding zero-point cyclotron energy. The zero-point cyclotron energy is approximately 7.4×10^{-4} for $B = 1.0$. For the considered electronic ground states of the manifolds $\sigma_g, \ldots, \mu_g$ for $B = 1.0$ we obtain harmonic potential energies of the order of magnitude of 10^{-3}. For the excited magnetically dressed states of the manifolds $\sigma_g, \ldots, \gamma_g$, i.e., the $2\sigma_g, 3\sigma_g, 4\sigma_g, 2\pi_u, \ldots, 2\gamma_g$ states, we obtain harmonic ground-state energies ranging from 10^{-3} to 10^{-4}. The estimated vibrational ground-state energies for each adiabatic electronic potential-energy curve of the considered "bonding" states of the manifolds $\sigma_g, \ldots, \mu_g$ are therefore much smaller than the depth of the corresponding wells. Hence many vibrational states can exist in these wells, i.e., the so-called "bonding" states of the H_2^+ ion in a strong magnetic field $B = 1.0$ are, within the adiabatic picture, stable.

TABLE II. The equilibrium internuclear distances R_{eq}, the electronic energy at the equilibrium distance $\varepsilon_T(R_{eq})$, and the dissociation energies ε_D of the bonding $\gamma, \eta, \ldots, \mu$ states ($m = -4, \ldots, -10$) in the presence of a magnetic field with $B = 0.01, 0.1, 1.0$.

| State	Magnetic quantum number	R_{eq}	ε_T	ε_D
		$B = 0.01$		
$1\gamma_g$	-4	40.4	$-0.037\,952$	2.828×10^{-4}
$1\eta_u$	-5	49.5	$-0.032\,369$	1.796×10^{-4}
$1\iota_g$	-6	57.4	$-0.028\,757$	1.318×10^{-4}
$1\varphi_u$	-7	64.1	$-0.026\,167$	0.963×10^{-4}
$1\kappa_g$	-8	70.3	$-0.024\,203$	0.766×10^{-4}
$1\lambda_u$	-9	75.9	$-0.022\,643$	0.653×10^{-4}
$1\mu_g$	-10	81.1	$-0.031\,259$	0.529×10^{-4}
		$B = 0.10$		
$1\gamma_g$	-4	17.59	$-0.100\,359$	3.548×10^{-3}
$1\eta_u$	-5	19.66	$-0.089\,757$	2.423×10^{-3}
$1\iota_g$	-6	21.51	$-0.082\,018$	2.018×10^{-3}
$1\varphi_u$	-7	23.21	$-0.076\,035$	1.679×10^{-3}
$1\kappa_g$	-8	25.22	$-0.071\,227$	1.599×10^{-3}
$1\lambda_u$	-9	26.81	$-0.067\,248$	1.472×10^{-3}
$1\mu_g$	-10	28.26	$-0.063\,883$	1.372×10^{-3}
		$B = 1.00$		
$1\gamma_g$	-4	6.55	$-0.289\,95$	2.376×10^{-2}
$1\eta_u$	-5	7.22	$-0.262\,50$	2.031×10^{-2}
$1\iota_g$	-6	7.82	$-0.241\,97$	1.800×10^{-2}
$1\varphi_u$	-7	8.35	$-0.225\,58$	1.611×10^{-2}
$1\kappa_g$	-8	8.86	$-0.212\,45$	1.480×10^{-2}
$1\lambda_u$	-9	9.35	$-0.201\,32$	1.362×10^{-2}
$1\mu_g$	-10	9.80	$-0.191\,82$	1.266×10^{-2}
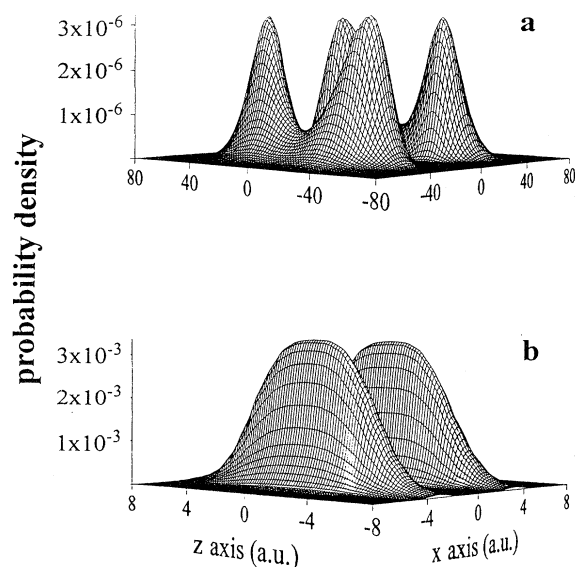
FIG. 3. (a) The electronic probability density distribution of the $6h\eta_u$ state in the absence of a magnetic field and for an internuclear distance of 80. (b) The electronic probability density distribution of the corresponding magnetically dressed $1\eta_u$ state at $R_{eq} = 7.22$.

5. Estimation of the center of mass motion effects

The above-discussed effects of a magnetic field on the electronic structure of the H_2^+ ion are based on the assumption of infinitely heavy nuclei, i.e., the applicability of the fixed-nuclei electronic Hamiltonian. However, as already discussed in Sec. II the center of mass motion of the H_2^+ ion couples to the electronic degrees of freedom if a magnetic field is present. In order to ensure that our fixed-nuclei approach is valid for the magnetically dressed states investigated we have to estimate the coupling of the center of mass motion of the H_2^+ ion to the corresponding electronic states. In Sec. II the relevant quantity κ [see Eq. (3)], which gives us the strength of the coupling of the center of mass and the electronic motion, has been introduced. Remember, if κ is much smaller than unity the coupling between different states of the collective and electronic motion is negligible.

We have calculated the values of κ according to Eq. (3) for all considered "bonding" states at their equilibrium distances and for the lowest Landau states with the quantum numbers $N \leq 2$, $|\mu| \leq 2$ as well as for several magnetic field strengths, i.e., $B = 0.01, 0.1$, and 1.0. For magnetic field strengths less than $B = 1.0$ the calculated values of κ are less than 10^{-4}, i.e., much smaller than one. This means that the influence of the coupling between the collective and electronic motion on the considered "bonding" states in a magnetic field with a field strength less than or equal to 0.1 is negligible. In the case of a magnetic field with $B = 1.0$ we obtained values of κ ranging from 10^{-4} to 10^{-2}. The cases for which κ is less than or of the order of magnitude of 10^{-3} occur for all considered molecular electronic states of the manifolds $\sigma_g, \ldots, \eta_u$ and for Landau states with the quantum numbers $N \leq 2$,

$|\mu| \leq 2$. The influence of the coupling between the center of mass and electronic motion is therefore also negligible for these states. With increasing degree of excitation of the molecular electronic states, i.e., increasing magnetic quantum number $|m|$ and/or increasing label n, and/or increasing degree of excitation of the Landau states, the values of κ increase rapidly (see Table III, which contains an extraction of our calculated values of κ for the electronic states $1\iota_g, \ldots, 1\mu_g$ and for a field strength of $B = 1.0$). For example, for the coupling between the Landau states $N = 2, \mu = 2$ and $N' = 2, \mu' = 1$ and the molecular electronic states $1\lambda_u$ and $1\mu_g$ the values of κ are approximately 2.3×10^{-2}. Values of κ of the order of magnitude of 10^{-2} indicate that corrections due to the coupling of the collective and electronic degrees of freedom become important. From our calculation of the parameter κ we therefore conclude that the coupling of the collective and electronic motion starts to become relevant at a field strength of $B = 1.0$ for the "bonding" molecular states with $|m| \geq 9$ and already for low-lying Landau orbitals of the center of mass motion. For the majority of the magnetically dressed "bonding" states considered, i.e., for the states with magnetic quantum numbers $|m| \leq 8$, the mixing of the wave functions due to the cou-

TABLE III. The calculated values of κ (see text) are given for the Landau states $N \leq 2, |\mu| \leq 2$ and the electronic ground states of the manifolds with the magnetic quantum numbers $m = -4, \ldots, -10$ and for a magnetic field strength $B = 1.0$.

Landau quantum numbers		Electronic states		Parameter
$N\mu$	$N'\mu'$	nm^P	$nm'^{P'}$	κ
00	01	$1\gamma_g$	$1\eta_u$	3.078×10^{-4}
01	02			6.156×10^{-4}
11	12			9.234×10^{-4}
21	22			1.231×10^{-3}
00	01	$1\eta_u$	$1\iota_g$	9.466×10^{-4}
01	02			1.893×10^{-3}
11	12			2.839×10^{-3}
21	22			3.786×10^{-3}
00	01	$1\iota_g$	$1\varphi_u$	2.824×10^{-3}
01	02			5.648×10^{-3}
11	12			9.045×10^{-3}
21	22			1.129×10^{-2}
00	01	$1\varphi_u$	$1\kappa_g$	1.085×10^{-4}
01	02			2.171×10^{-4}
11	12			3.528×10^{-4}
21	22			4.341×10^{-4}
00	01	$1\kappa_g$	$1\lambda_u$	4.518×10^{-3}
01	02			9.037×10^{-3}
11	12			1.492×10^{-2}
21	22			1.807×10^{-2}
00	01	$1\lambda_u$	$1\mu_g$	5.624×10^{-3}
01	02			1.124×10^{-2}
11	12			1.888×10^{-2}
21	22			2.249×10^{-2}

pling is negligible for the lowest Landau levels with $N \leq 2, \mu \leq 2$. These Landau levels of the center of mass motion correspond to a temperature of the order of magnitude of 100 K. It is, of course, also possible to obtain for the low-lying electronic states a strong interaction between the electronic and center of mass motion by further increasing the quantum numbers N and/or μ, i.e., by choosing highly excited Landau levels of the center of mass motion of the ion, and/or by further increasing the field strength.

B. The magnetically dressed antibonding states

Let us now consider the influence of a strong magnetic field on the so-called "antibonding" states. In the sense of the above-discussed correlation (see Sec. IV) between the molecular states of the H_2^+ ion in the field-free space and those in the presence of a magnetic field, we again compare the lowest three states of each considered "antibonding" manifold in the absence of a magnetic field, i.e., the states $2p\sigma_u, 4f\sigma_u, 3p\sigma_g, 3d\pi_g, \ldots$, with their corresponding counterparts $1\sigma_u, 2\sigma_u, 3\sigma_u, 1\pi_g, \ldots$ in the presence of a magnetic field. In field-free space the potential-energy curves of the ground states of the "antibonding" manifolds with the magnetic quantum numbers $|m| = 0, \ldots, 10$, i.e., the $2p\sigma_u, 3d\pi_g, \ldots, 12n\mu_u$ states, exhibit a purely repulsive behavior [see Table IV(a)]. In previous investigations (see Refs. [17,18] and [27,28]) it was shown that the potential-energy curves of the corresponding magnetically dressed counterparts, i.e., $1\sigma_u, 1\pi_g, \ldots, 1\mu_u$ states, show above some critical field strength shallow minima. For a field strength of $B = 1.0$ the depth of the shallow potential wells of these "antibonding" ground states ranges from 5.40×10^{-4} a.u. for the $1\sigma_u$ state to 3×10^{-6} for the $1\mu_u$ state [see Table IV(b)]. All these energies are smaller than the cyclotron energy of the nuclear relative motion and therefore these "antibonding" ground states are supposed to be unbound. The potential-energy curves of the first excited states of the manifolds $\sigma_u, \pi_g, \ldots, \gamma_u$ exhibit also in the absence of a magnetic field potential-energy wells. The depths of these potential wells are of the order of magnitude of 10^{-3} [see Table IV(a) for a complete list of the dissociation energies and equilibrium distances of these "antibonding" states of the H_2^+ ion in field-free space]. If we switch on a magnetic field $B = 1.0$ we obtain for the corresponding magnetically dressed states an overall decrease of the equilibrium distances and a decrease of the dissociation energies for the $2\sigma_u, 2\pi_g, 2\delta_u$ states while the dissociation energies of the $2\phi_g$ and $2\gamma_u$ states increase. For example, the $4f\sigma_u$ state in the field-free space has an equilibrium distance of 21.0 and a dissociation energy of 5.40×10^{-3}. For the corresponding counterpart in the presence of a magnetic field $B = 1.0$ we obtain a dissociation energy of 1.94×10^{-3} and an equilibrium distance of 16.5 [see Table IV(b) for a complete list of the calculated dissociation energies and equilibrium distances of the "antibonding" states of the H_2^+ ion in a magnetic field $B = 1.0$]. The depths of the potential wells of the energy curves of these magnetically dressed first excited states are of the order of magnitude of 10^{-3}.

The potential-energy curves of the second excited magnetically dressed states, i.e., the $3\sigma_u, 3\pi_g, 3\delta_u$ states, also exhibit potential wells. The depths of these wells are of the same order of magnitude as those of the first excited states. The potential-energy curves of their corresponding field-free counterparts, i.e., the $3p\sigma_u, 4d\pi_g, 5f\delta_u$

TABLE IV. The equilibrium internuclear distances R_{eq}, the electronic energy at the equilibrium distance $\varepsilon_T(R_{eq})$, and the dissociation energies ε_D of the antibonding $\sigma, \pi, \ldots, \mu$ states ($m = 0, \ldots, -10$) (a) in the absence of a magnetic field and (b) in the presence of a magnetic field $B = 1.0$.

State	R_{eq}	$\varepsilon_T(R_{eq})$	ε_D
		(a)	
$2p\sigma_u$		purely repulsive	
$4f\sigma_u$	21.0	-1.304×10^{-1}	5.40×10^{-3}
$3p\sigma_u$		purely repulsive	
$6h\sigma_u$	41.5	-6.056×10^{-2}	5.00×10^{-3}
$3d\pi_g$		purely repulsive	
$5g\pi_g$	35.5	-5.822×10^{-2}	2.66×10^{-3}
$4d\pi_g$		purely repulsive	
$7i\pi_g$	60.0	-3.418×10^{-2}	2.93×10^{-3}
$4f\delta_u$		purely repulsive	
$6h\delta_u$	54.0	-3.269×10^{-2}	1.44×10^{-3}
$5f\delta_u$		purely repulsive	
$8j\delta_u$	83.0	-2.183×10^{-2}	1.83×10^{-3}
$5g\phi_g$		purely repulsive	
$7i\phi_g$	76.0	-2.083×10^{-2}	8.30×10^{-4}
$6h\gamma_u$		purely repulsive	
$8j\gamma_u$	104.0	-1.436×10^{-2}	4.80×10^{-4}
		(b)	
$1\sigma_u$	9.6	-8.300×10^{-1}	5.40×10^{-4}
$2\sigma_u$	16.5	-2.618×10^{-1}	1.94×10^{-3}
$3\sigma_u$	24.0	-1.619×10^{-1}	1.64×10^{-3}
$4\sigma_u$	35.0	-9.257×10^{-2}	2.39×10^{-3}
$1\pi_g$	13.5	-4.567×10^{-1}	2.21×10^{-4}
$2\pi_g$	19.5	-2.082×10^{-1}	1.62×10^{-3}
$3\pi_g$	28.0	-1.272×10^{-1}	1.69×10^{-3}
$4\pi_g$	39.4	-8.128×10^{-2}	1.94×10^{-3}
$1\delta_u$	16.0	-3.532×10^{-1}	1.79×10^{-4}
$2\delta_u$	21.5	-1.815×10^{-1}	1.50×10^{-3}
$3\delta_u$	30.5	-1.132×10^{-1}	1.69×10^{-3}
$4\delta_u$			
$1\phi_g$	18.0	-3.001×10^{-1}	1.46×10^{-4}
$2\phi_g$	23.0	-1.644×10^{-1}	1.42×10^{-3}
$1\gamma_u$	19.5	-2.663×10^{-1}	1.17×10^{-4}
$2\gamma_u$	24.0	-1.522×10^{-1}	1.35×10^{-3}
$1\eta_g$	20.5	-2.423×10^{-1}	0.90×10^{-4}
$1\iota_u$	22.0	-2.240×10^{-1}	0.80×10^{-4}
$1\varphi_g$	23.0	-2.095×10^{-1}	0.60×10^{-4}
$1\kappa_u$	24.5	-1.977×10^{-1}	0.50×10^{-4}
$1\lambda_g$	23.0	-1.878×10^{-1}	0.13×10^{-4}
$1\mu_u$	26.0	-1.792×10^{-1}	0.03×10^{-4}

states, show a purely repulsive behavior. All dissociation energies of these excited magnetically dressed "antibonding" states for a field strength $B = 1.0$ are roughly two times larger than the cyclotron energy of the nuclear motion. By our simple estimation of the vibrational ground-state energy in the presence of a magnetic field it is therefore not possible to decide whether vibrational states do exist in the potential wells of the above-discussed excited magnetically dressed "antibonding" states. A more accurate determination of the vibrational levels which goes beyond the harmonic approximation of the well would be necessary in order to decide on the stability of the excited magnetically dressed "antibonding" states for $B = 1.0$. In addition, we want to mention that the overall accuracy of the dissociation energies of the "bonding" states is roughly 0.1% whereas the typical accuracy of the corresponding values of the "antibonding" states is of the order of magnitude of 1%.

C. Remarks on nonparallel configurations

In the present paper we have investigated a large number of electronic states of the H_2^+ ion in a homogeneous magnetic field for the case of parallel internuclear and magnetic field axes. The symmetries for this parallel configuration are, as we mentioned in Sec. II, parity and the rotational invariance around the internuclear axis. However, for the general case $0° < \Theta < 90°$ the only remaining symmetry is parity. Therefore the crossings of the potential-energy curves of the electronic states with different magnetic quantum numbers but the same parity in the parallel configuration turn into avoided crossings if the internuclear axis is inclined with respect to the magnetic field axis. In Fig. 4 we have illustrated the above-described situation for the potential-energy curves of the eight lowest states of the H_2^+ ion in a magnetic field of

$B = 1.0$ with gerade parity. The case $\Theta = 0°$ is shown in Fig. 4(a). Apart from the well-known crossing of the potential-energy curves of the $1\pi_g$ and $1\delta_g$ states [16] the number of crossings increases rapidly with increasing degree of excitation of the molecular electronic states. In Fig. 4(b) the potential-energy curves of the corresponding electronic states are illustrated for an angle $\Theta = 5°$. The potential-energy curves of the 2_g and 3_g states are now well separated, i.e., we obtain a strong repulsion of the $1\pi_g$-$1\delta_g$ states if we change the configuration from $\Theta = 0°$ to a small nonvanishing angle Θ. In contrast to this the avoided crossing of the 4_g and 5_g states at approximately 10.25, which evolves from the crossing of the $2\sigma_g$ and $1\phi_g$ states at $\Theta = 0°$, is very narrow. However, a detailed study of the full potential-energy surfaces of the excited states of the H_2^+ ion in a strong magnetic field goes beyond the scope of the present paper and will be the task of future investigations.

Finally, a remark on the numerical effort of our calculations is appropriate. A rather large number of optimized atomic orbital basis functions was necessary to obtain the above results: The typical number of basis functions we used was roughly 200. By using a Silicon Graphics Indigo R4000 workstation the average CPU time to get one point, i.e., for one internuclear distance R, was between 2 and 6 h (depending on the number of basis functions and the quantum numbers of the considered subspace). The total CPU time of our investigation therefore amounts to one and a half years on the above computer.

VI. BRIEF SUMMARY

We have studied a large number of excited magnetically dressed states of the H_2^+ ion for parallel internuclear
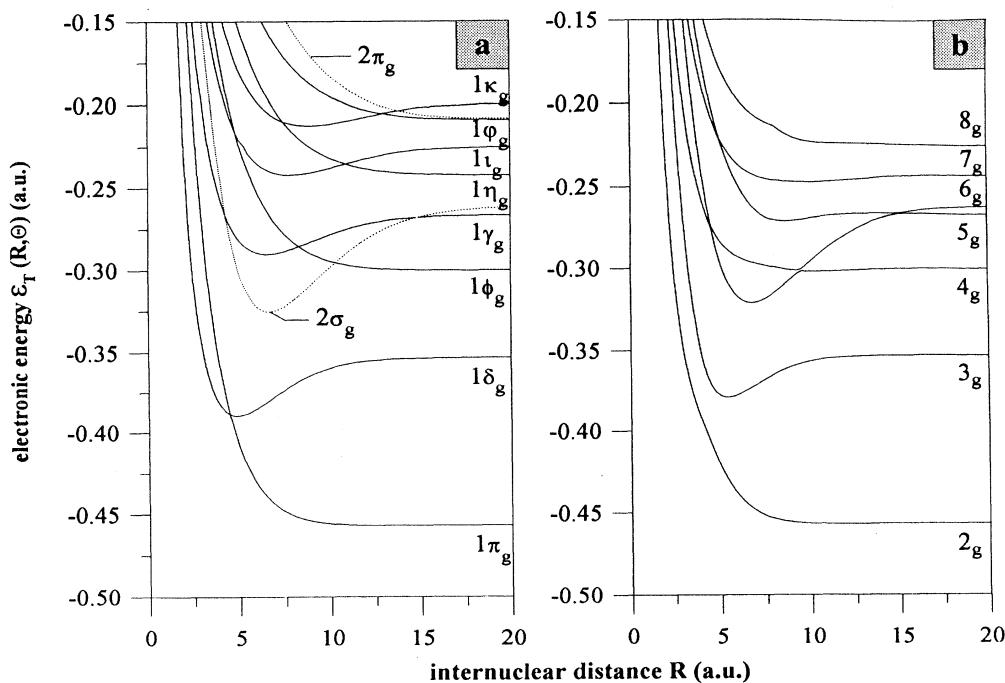
FIG. 4. Adiabatic potential-energy curves for excited electronic states of the H_2^+ ion with gerade parity in a strong magnetic field $B = 1.0$ plotted as functions of the internuclear distance R for (a) $\Theta = 0°$ and (b) $\Theta = 5°$.

and magnetic field axes. The key ingredient for our extensive numerical calculations of the molecular electronic states and potential-energy curves in the fixed-nuclei approximation was a recently established and optimized basis set of generalized atomic orbitals. In order to understand the influence of the magnetic field on the chemical bond of excited molecular states we performed a detailed comparison of the electronic probability distributions and potential-energy curves in field-free space with those in the presence of the external field. First we investigated the so-called "bonding" states. In the absence of a magnetic field the potential-energy curves of the second excited states of the manifolds $\sigma_g, \pi_u, \delta_g$ as well as the ground states of the manifolds $\eta_u, \ldots, \mu_g$ exhibit a purely repulsive behavior. If we switch on a typical strong field of $B = 1.0$ a.u. all potential-energy curves of the considered "bonding" states and, in particular, the second excited states of the manifolds $\sigma_g, \pi_u, \delta_g$ as well as the ground states of the manifolds $\eta_u, \ldots, \mu_g$ exhibit well-pronounced potential wells. The reason for the drastic changes in the latter potential-energy curves in the presence of a magnetic field is, apart from the overall enhancement of the absolute values of the electronic density in the plane perpendicular to the magnetic field axis, the appearance of a global maximum of the probability density on or close to the internuclear axis and between both nuclei. These density maxima do not occur in the field-free case. By a harmonic approximation of the wells we could show that in all cases considered the vibrational ground-state energy is much smaller than the depth of the corresponding well and therefore many vibrational states exist in these wells.

Since the above-discussed effects of the H_2^+ ion are based on the fixed-nuclei approximation we have to estimate whether the corrections beyond this approximation, i.e., the coupling between the collective and electronic motion of the H_2^+ ion and the mass corrections, are small. We showed that the quantity κ, which is a measure for the strength of the coupling for the lowest Landau levels of the center of mass motion is much smaller than unity. Exceptions are the electronic $1\lambda_u$ and $1\mu_g$ states for which κ is of the order of magnitude of a few times 10^{-2}, i.e., for these states the coupling to the center of mass is no longer a tiny correction and increases rapidly with increasing excitation of the Landau levels.

The main result of our investigation of the so-called "bonding" states is therefore the fact that all considered states of the manifolds $\sigma_g, \ldots, \kappa_g$ and, in particular, also those whose corresponding counterparts are unbound in the absence of a magnetic field, become stable with respect to dissociation $H_2^+ \rightarrow H + p$ through the presence of a strong field.

In contrast to the potential-energy curves of the bonding states the potential-energy curves of the so-called antibonding states of the manifolds $\sigma_u, \ldots, \mu_u$ exhibit in the presence of a strong field $B = 1.0$ only shallow minima. The depths of the potential wells of the ground states of the considered manifolds are in each case smaller than the corresponding zero-point cyclotron energy of the nuclear motion. Hence these magnetically dressed states are physically unbound. The depth of the con-

sidered excited states of the manifolds $\sigma_u, \ldots, \gamma_u$ are roughly two times larger than the corresponding zero-point cyclotron energy of the nuclear motion. Within a simple approximation of the potential wells by a harmonic potential and an estimation of the vibrational ground-state energy in this harmonic potential under the influence of the external magnetic field it is not possible to decide whether vibrational states can exist in the potential wells of the excited antibonding states considered.

Finally we showed the existence of a large number of crossings for the potential-energy curves for $\Theta = 0°$ which turn into avoided crossings if the internuclear axis is inclined with respect to the magnetic field axis. This fact indicates the complexity of the topology of the full electronic potential surfaces $\varepsilon = \varepsilon(R, \Theta)$ which becomes particularly relevant for higher excited states. An investigation of the topology of the potential surfaces of the excited states in a magnetic field is a challenging task from both the numerical as well as the physical point of view and is left to future investigations.

ACKNOWLEDGMENTS

APPENDIX

In order to describe the construction of our molecular orbitals with the optimized basis functions given in Ref. [27], some preliminary remarks concerning these optimized atomic orbitals are necessary.

For vanishing pseudomomentum which implies a constant angular momentum L_z the dynamics of the hydrogen atom in a strong homogeneous magnetic field depends only on the transversal coordinate $\rho = (x^2 + y^2)^{1/2}$ and the z coordinate parallel to the magnetic field. For this reason the atomic orbitals which were used to perform the optimization are given in cylindrical coordinates and contain only two variational parameters, α and β. They take on the following appearance:

$$\Omega_{s,t}^{m_a P_a}(\rho, z, \varphi, \underline{\alpha}) = \rho^{m_a + 2s} z^t \exp\{-\alpha\rho^2 - \beta z^2\}$$

$$\times \exp\{im_a\varphi\} , \qquad (A1)$$

where m_a and $P_a = (-)^{m_a}(-)^t$ denote the magnetic quantum number and parity of the atom, respectively. s and t are positive integers and characterize the type of atomic orbitals in a given subspace $m_a^{P_a}$.

Since we use Cartesian atomic orbitals for the construction of our molecular orbitals, we have to transform the atomic orbitals (A1) into the corresponding Cartesian basis functions. This follows via the simple identity

$$\rho^{m_a+2s}\exp\{im_a\varphi\}=\sum_{\sigma}^{|m_a|}\sum_{\tau}^{s}\begin{bmatrix}|m_a|\\\sigma\end{bmatrix}\begin{bmatrix}s\\\tau\end{bmatrix}$$

$$\times x^{|m_a|-\sigma+2(s-\tau)}$$

$$\times(i\pm)^{\sigma}y^{\sigma+2\tau}\ .\qquad(A2)$$

Hence we obtain by the transformation (A2), in general, a set of Cartesian atomic orbitals characterized by the index i with the same variational parameters α and β but different triads $\mathbf{n}_{\sigma\tau,i}=(n_{x,i}^{\sigma\tau},n_{y,i}^{\sigma\tau},n_{z,i}^{\sigma\tau})$:

$$\Omega_{\mathbf{n}_{\sigma\tau,i}}^{P_a}(\mathbf{r},\underline{\alpha}_i)=x^{n_{x,i}^{\sigma\tau}}y^{n_{y,i}^{\sigma\tau}}z^{n_{z,i}^{\sigma\tau}}$$

$$\times\exp\{-\alpha_i(x^2+y^2)-\beta_iz^2\}\ ,\qquad(A3)$$

with

$$n_{x,i}^{\sigma\tau}=|m_a|-\sigma+2(s-\tau)\ ,$$

$$n_{y,i}^{\sigma\tau}=\sigma+2\tau\ ,$$

$$n_{z,i}^{\sigma\tau}=t\ .$$

The Cartesian atomic orbitals are still eigenfunctions to the atomic parity operator $P_a=(-)^{n_{x,i}^{\sigma\tau}+n_{y,i}^{\sigma\tau}+n_{z,i}^{\sigma\tau}}$, but obviously not to the atomic angular momentum operator L_z.

For the case of the H_2^+ ion in a homogeneous magnetic field with parallel internuclear and magnetic field axes the atomic orbitals (A3), centered at the positions of the nuclei, read in the molecular coordinate system, which has its origin in the center of mass of nuclei, as follows:

$$\phi_{\mathbf{n}_{\sigma\tau,i}}(\mathbf{r},\underline{\alpha}_i,\pm R/2)=x^{n_{x,i}^{\sigma\tau}}y^{n_{y,i}^{\sigma\tau}}(z\mp R/2)^{n_{z,i}^{\sigma\tau}}$$

$$\times\exp\{-\alpha_i(x^2+y^2)$$

$$-\beta_i(z\mp R/2)^2\}\ ,\qquad(A4)$$

where R is the internuclear distance.

The molecular orbitals $\phi_{\mathbf{n}_{\sigma\tau,i}}^{P}$ which are eigenfunctions of the molecular parity operator P can be constructed from the functions (A4) by defining

$$\Phi_{\mathbf{n}_{\sigma\tau,i}}^{P}(\mathbf{r},\underline{\alpha}_i,R)=\phi_{\mathbf{n}_{\sigma\tau,i}}(\mathbf{r},\underline{\alpha}_i,R/2)$$

$$+PP_a\phi_{\mathbf{n}_{\sigma\tau,i}}(\mathbf{r},\underline{\alpha}_i,-R/2)\ .\qquad(A5)$$

Molecular orbitals which are also eigenfunctions to the z component L_z of the molecular angular momentum operator can be obtained by linear combination of the molecular orbitals (A5) belonging to a set i. For a given molecular magnetic quantum number m, the components $n_{x,i}^{\sigma\tau}$ and $n_{y,i}^{\sigma\tau}$ of the triad $\mathbf{n}_{\sigma\tau,i}$ have to satisfy the condition

$$|m|+2k=n_{x,i}^{\sigma\tau}+n_{y,i}^{\sigma\tau}\ ,\qquad(A6)$$

where k is a positive integer. Analogous to the "atomic" equation (A2) we may construct the molecular eigenfunctions of the operator L_z by combining

$$\Phi_i^{\pm m,P}(\mathbf{r},\underline{\alpha}_i,R)=\sum_{\mu}^{|m|}\sum_{\nu}^{k}\begin{bmatrix}|m|\\\mu\end{bmatrix}\begin{bmatrix}k\\\nu\end{bmatrix}(\pm i)^{\mu}\Phi_{\mathbf{n}_{\mu\nu,i}}^{P}(\mathbf{r},\underline{\alpha}_i,R)$$

$$=\sum_{\mu}^{|m|}\sum_{\nu}^{k}\begin{bmatrix}|m|\\\mu\end{bmatrix}\begin{bmatrix}k\\\nu\end{bmatrix}(\pm i)^{\mu}[\phi_{\mathbf{n}_{\mu\nu,i}}(\mathbf{r},\underline{\alpha}_i,R/2)+PP'\phi_{\mathbf{n}_{\mu\nu,i}}(\mathbf{r},\underline{\alpha}_i,-R/2)]\ ,\qquad(A7)$$

where μ,ν are the molecular summation indices (they are, in general, not equal to the atomic indices σ,τ). Each element of the calculated Hamiltonian matrix is the expectation value of the fixed-nuclei Hamiltonian (2) with respect to a molecular orbital of the form (A7).

[1] C. P. de Melo, R. Ferreira, H. S. Brandi, and L. C. M. Miranda, Phys. Rev. Lett. 37, 676 (1976).
[2] C. S. Lai and B. Suen, Can. J. Phys. 55, 609 (1977).
[3] L. C. de Melo, T. K. Das, R. C. Ferreira, L. C. M. Miranda, and H. S. Brandi, Phys. Rev. A 18, 13 (1978).
[4] R. K. Bhaduri, Y. Nogami, and C. S. Warke, Astrophys. J. 217, 324 (1977).
[5] C. S. Lai, Can. J. Phys. 55, 1013 (1977).
[6] J. M. Peek and J. Katriel, Phys. Rev. A 21, 413 (1980).
[7] M. S. Kaschiev, S. I. Vinitsky, and F. R. Vukajlovic, Phys. Rev. A 22, 557 (1980).
[8] J. Ozaki and Y. Tomishima, J. Phys. Soc. Jpn. 49, 1497 (1980); Phys. Lett. 82A, 449 (1981).
[9] D. M. Larsen, Phys. Rev. A 25, 1295 (1982).
[10] S. A. Maluendes, F. M. Fernandez, and E. A. Castro, Phys. Rev. A 28, 2059 (1983).
[11] G. Wunner, H. Herold, and H. Ruder, Phys. Lett. 88A, 344 (1982).
[12] V. K. Khersonskij, Astrophys. Space Sci. 87, 61 (1982); 98, 255 (1984); 103, 357 (1984); 117, 47 (1985); Opt. Spektrosk. 55, 825 (1983) [Opt. Spectrosc. (USSR) 55, 495 (1983)].
[13] J. C. le Gouillou and J. Zinn-Justin, Ann. Phys. (N.Y.) 154, 440 (1984).
[14] M. Vincke and D. Baye, J. Phys. B 18, 167 (1985).
[15] D. R. Brigham and J. M. Wadehra, Astrophys. J 317, 865 (1987).
[16] U. Wille, J. Phys. B 20, L417 (1987); Phys. Rev. A 38, 3210 (1988).
[17] J. Ozaki and Y. Hayashi, J. Phys. Soc. Jpn. 58, 3564 (1989).

[18] J. Ozaki, J. Phys. Soc. Jpn. **62**, 15 (1993).

[19] Y. E. Lozovik and A. V. Klyuchnik, Phys. Lett. **66A**, 282 (1978).

[20] M. Zaucer and A. Azman, Phys. Rev. A **18**, 1320 (1978).

[21] C. S. Warke and A. K. Dutta, Phys. Rev. A **16**, 1747 (1977).

[22] A. V. Turbiner, Pis'ma Zh. Eksp. Teor. Fiz. **38**, 510 (1983) [JETP Lett. **38**, 618 (1983)].

[23] S. Basile, F. Trombetta, and G. Ferrante, Nuovo Cimento **9**, 457 (1987).

[24] T. S. Monteiro and K. T. Taylor, J. Phys. B **22**, L191 (1989); **23**, 427 (1990).

[25] M. Demeur, P. H. Heenen, and M. Godefroid, Phys. Rev. A **49**, 176 (1994); A. M. Abrahams and S. L. Shapiro, Astrophys. J. **382**, 233 (1991); A. V. Korolev and M. A. Liberman, Phys. Rev. A **45**, 1762 (1992); D. Lai, E. E. Salpeter, and S. L. Shapiro, *ibid*. **45**, 4832 (1992).

[26] P. Schmelcher and L. S. Cederbaum, Phys. Rev. A **37**, 672 (1988).

[27] U. Kappes and P. Schmelcher, J. Chem. Phys. **100**, 2878 (1994).

[28] U. Kappes, P. Schmelcher, and T. Pacher, Phys. Rev. A **50**, 3775 (1994).

[29] J. E. Avron, I. W. Herbst, and B. Simon, Ann. Phys. (N.Y.) **114**, 431 (1978).

[30] D. Baye and M. Vincke, Phys. Rev. A **42**, 31 (1990).

[31] P. Schmelcher and L. S. Cederbaum, Phys. Rev. A **43**, 287 (1991).

[32] P. Schmelcher, L. S. Cederbaum, and U. Kappes, *Conceptual Trends in Quantum Chemistry* (Kluwer, Dordrecht, 1994).

[33] W. E. Lamb, Phys. Rev. **85**, 259 (1959).

[34] B. R. Johnson, J. O. Hirschfelder, and K. H. Yang, Rev. Mod. Phys. **55**, 109 (1983).

[35] P. Schmelcher, L. S. Cederbaum, and H. D. Meyer, Phys. Rev. **38**, 6066 (1988); J. Phys. B **21**, L445 (1988).

[36] T. Detmer, P. Schmelcher, and L. S. Cederbaum (unpublished).

[37] M. Kotani, K. Ohno, and K. Kayama, in *Quantum Mechanics of Electronic Structure of Simple Molecules*, edited by S. Flügge, Handbüch der Physik Vol. XXXVII/2 (Springer-Verlag, Berlin, 1961).

[38] S. P. Alliluev and A. V. Matveenko, Zh. Eksp. Teor. Fiz. **51**, 1873 (1966) [Sov. Phys. JETP **24**, 1260 (1967)].

[39] D. R. Bates, K. Ledsham, and A. L. Stewart, Philos. Trans. R. Soc. London, Ser. A **246**, 215 (1953); D. R. Bates and R. H. G. Reid, Adv. At. Mol. Phys. **4**, 13 (1968).

[40] P. Schmelcher and L. S. Cederbaum, Phys. Rev. A **41**, 4936 (1990).